PHYSICAL REVIEW B **69**, 104508 (2004)

First-principles study of $HgBa_2Ca_{n-1}Cu_nO_{2n+2}$ under pressure

T. Thonhauser,[1] H. Auer,[2] E. Ya. Sherman,[2] and C. Ambrosch-Draxl[2]
[1]*Department of Physics, Pennsylvania State University, University Park, Pennsylvania 16802, USA*
[2]*Institut für Theoretische Physik, Universität Graz, Universitätsplatz 5, 8010 Graz, Austria*

(Received 17 October 2003; published 17 March 2004)

Using first-principles calculations, we investigate structural and electronic properties of $HgBa_2Ca_{n-1}Cu_nO_{2n+2}$ cuprates for $n=1,2,3,4,$ and pressure in the range from 0 to 15 GPa. All four compounds are compared to each other with respect to structural data, band structure, partial charges, and the dependence of these properties upon composition n and pressure is pointed out. Furthermore, the analysis of the partial charges allows, in particular, examination of charges within the CuO_2 layers. Using this method, we focus on the creation of holes in these layers and their dependence on composition and pressure. Our results show that a direct correlation between the hole content and the superconducting transition temperature exists.

DOI: 10.1103/PhysRevB.69.104508 PACS number(s): 74.25.Jb, 74.25.Ld, 71.15.Mb

I. INTRODUCTION

The excellent superconducting properties of the Hg-based cuprates $HgBa_2Ca_{n-1}Cu_nO_{2n+2}$ were discovered in 1993 and their transition temperatures T_c are the highest observed.[1,2] The structure of all these compounds is relatively simple and, furthermore, T_c depends strongly on parameters such as doping, number of CuO_2 layers n, and pressure.[3] Thus, this homologous series is a very good candidate for studies. In order to better understand the connection between structural aspects, the electronic structure, and superconductivity we performed first-principle calculations on $HgBa_2Ca_{n-1}Cu_nO_{2n+2}$ for $n=1,2,3,4$ and pressure in the range from 0 to 15 GPa.

The experimentally observed transition temperature for $n=1$ is 97 K, which is the highest of all single-layered compounds. This value can be increased by inserting one more CuO_2 layer and the critical temperature for $n=2$ becomes 127 K.[4] Inserting another layer raises T_c again and 135 K is reported for $n=3$.[1] Including more than two layers does not lead to any further improvement. Instead, a decrease for $n=4,5,$ and 6 to 127 K, 110 K, and 107 K, respectively, is found.[5] However, the transition temperature increases again by applying pressure,[6–8] which is well known for Cu-containing superconductors with hole-type conductivity. In the case of $HgBa_2Ca_2Cu_3O_8$ under 30 GPa T_c was found to be 164 K, which is the highest ever measured.[9] This has led to a widespread interest in the physical properties of the homologous Hg-based series.

Calculations for some of the compounds mentioned can, for example, be found in Refs. 10–12. In the present paper we show results for a theoretical study of $n=1,2,3,4$. Since all our calculations are done on the same footing, a comparison of these compounds with one another is possible. Thereby, we focus on comparing structural data, band structures, partial charges, and the dependence of these properties upon composition and pressure. Furthermore, we investigate the creation of holes in the CuO_2 planes and analyze their connection to the superconducting transition temperature.

II. CRYSTAL STRUCTURE

All members of the Hg family crystallize in a tetragonal lattice with space group $P4/mmm$, where the c axis is perpendicular to the CuO_2 planes. These planes are the main building block of all these compounds and are responsible for the superconducting properties. A short notation for the different representatives is given according to the number n of CuO_2 layers as Hg-12$(n-1)n$. Thereby, "1" stands for one Hg and "2" for two Ba atoms in each cell. The $n-1$ Ca atoms, and the n CuO_2 planes further determine this nomenclature. While values of $n=1$ to 6 are possible, we confined ourselves to a maximum of 4 and, henceforth, we will use the short notation Hg-1201, Hg-1212, Hg-1223, and Hg-1234. Pictures of the corresponding unit cells are shown in Fig. 1 where the layer structure becomes clearly visible. We may also refer to these compounds as one-, two-, three-, and four-layered systems. Experimental values for the lattice constants a and c can be found in Table I.

The Hg-1201 compound has five inequivalent atoms in its unit cell and eight total. Inserting one Ca atom and one CuO_2 layer leads to Hg-1212 with its 6 inequivalent atoms and 12 atoms total. Higher compounds are generated by adding further units of Ca atoms and CuO_2 planes. This way we get Hg-1223 (8 inequivalent atoms, 16 total) and Hg-1234 (9 inequivalent atoms, 20 total). The procedure influences mostly the c lattice parameter, while a is approximately the same for all systems. From the data in Table I it follows that the dependence of c on n can be approximated by $c(n)\approx 18+6(n-1)$ a.u.

The apical oxygen will in all four systems be referred to as O^a. Furthermore, the CuO_2 layers are counted ascending from bottom to top. Atoms in the first layer are therefore referred to as Cu^1 and O^1 and in the second layer as Cu^2 and O^2.

III. METHOD OF CALCULATION

Our calculations were performed within the full-potential linearized augmented plane-wave (FP-LAPW) method as implemented in the WIEN2K code.[16] Exchange and correlation effects are accounted for by the local-density approximation (LDA) parametrized by Perdew and Wang.[17] Parameters such as the density of the k mesh and $RK_{\max}$ were tested for convergence. The spheres radii for our calculations were chosen to be 2.1 a.u. (Hg), 2.3 a.u. (Ba), 1.9 a.u. (Cu), 1.2

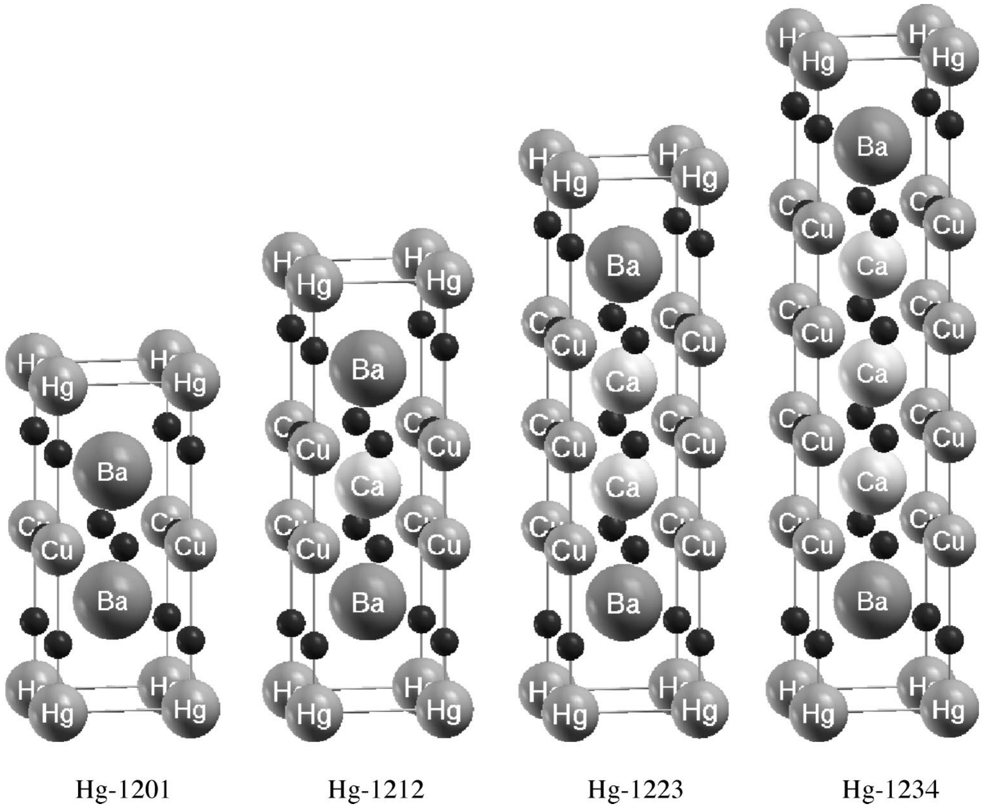

FIG. 1. Unit cells of the compounds Hg-1201, Hg-1212, Hg-1223, and Hg-1234. Little black spheres correspond to oxygen atoms. The apical oxygen will be denoted O^a in all four compounds. The CuO_2 layers are counted ascending from bottom to top. Atoms in the first layer are therefore referred to as Cu^1 and O^1 and in the second layer as Cu^2 and O^2.

a.u. (O), and 2.0 a.u. (Ca). Furthermore, all calculations for different number of layers and pressures were done with the same set of parameters, in order to make a comparison possible.

The LAPW method divides space into two regions: Spheres, which are centered around atoms, and the interstitial region in between the spheres. Within the spheres the wave function is expanded into spherical harmonics. In the case of convergence with self-consistency cycles, this expansion allows for the analyzation of the charge not only according to their atomic origin, but also with respect to their angular momentum decomposition in *l* and *m*. Charges can then be split up into, e.g., $p_x, p_y, p_z, d_{x^2-y^2}, d_{z^2}, d_{xy}, \ldots$. Note that the charges are not constant but depend on the freely chosen sphere sizes. This is important for studies under pressure, where the unit-cell volume decreases. It complicates the interpretation of the partial charges (see Sec. IV C), since the amount of charge (volume) lying within the spheres with respect to the total charge (volume) becomes larger. Nevertheless, the partial charges can still be used to study trends.

TABLE I. Experimental data for the Hg-1201, Hg-1212, Hg1223, and Hg-1234 systems under ambient pressure. Given are the unit cell volume *V*, the lattice constants *a* and *c* together with their ratio, and a reference to the corresponding experiment.

Compound	V [a.u.^{3}]	a [a.u.]	c [a.u.]	c/a	Ref.
Hg-1201	967.7	7.332	18.000	2.455	13
Hg-1212	1278.7	7.300	23.995	3.287	14
Hg-1223	1578.0	7.278	29.790	4.093	15
Hg-1234	1901.1	7.278	35.890	4.931	15

IV. RESULTS AND DISCUSSION

A. Structural data

We performed total-energy calculations for a grid of the lattice parameters *a* and *c* around the values of Table I. For each configuration the internal parameters, i.e., atomic forces, were relaxed. The resulting energy surface was then fitted to third order polynomials in *a* and *c*. From this parametrization we determined where the points of hydrostatic pressure in term of the lattice parameters are located. Results for the calculated parameters *a* and *c* are given in Table II for the compounds Hg-1201, Hg-1212, Hg-1223, and Hg-1234 under pressure.

The importance of structural properties for the superconducting mechanism is pointed out by Antipov and coworkers in great detail.[5] They found that the Cu-O in-plane distance influences the appearance of superconducting properties. In order to delocalize carriers in the partially filled conduction band, the Cu-O distance should be between 3.54 a.u. and 3.72 a.u. under ambient pressure. Note that twice the Cu-O distance equals the lattice parameter *a* only in case of planar layers.

TABLE II. Calculated structural data for Hg-1201, Hg-1212, Hg-1223, and Hg-1234 under pressure. Given are the pressure P, unit cell volume V, the lattice constants a, c, and their ratio c/a.

Compound	P [GPa]	V [a.u.^{3}]	a [a.u.]	c [a.u.]	c/a
Hg-1201	0	920.5	7.2071	17.7212	2.459
	5	856.0	7.0844	17.0555	2.408
	10	798.9	6.9769	16.4123	2.352
	15	747.1	6.8804	15.7825	2.294
Hg-1212	0	1213.9	7.1674	23.6301	3.297
	5	1140.8	7.0706	22.8189	3.227
	10	1074.9	6.9844	22.0346	3.155
	15	1014.4	6.9060	21.2684	3.080
Hg-1223	0	1515.0	7.1654	29.5065	4.118
	5	1436.1	7.0877	28.5878	4.033
	10	1363.9	7.0178	27.6940	3.946
	15	1296.9	6.9539	26.8186	3.857
Hg-1234	0	1773.5	7.0888	35.2930	4.979
	5	1664.0	6.9824	34.1299	4.888
	10	1565.8	6.8866	33.0170	4.794
	15	1476.2	6.7987	31.9367	4.697

The calculated values for the lattice constants under ambient pressure can be compared to experimental data given in Table I. In case of Hg-1201, our calculated value for the optimal volume under zero pressure is about 4.8% smaller than the experimental one, which is within the boundaries of the well-known LDA overbinding. More important, however, is the c/a ratios match, which emphasizes the reliability of our calculations. The case is similar for the other systems: Hg-1212, Hg-1223, and Hg-1234. Although, the experiments get more complicated as the number of CuO_2 layers increases and problems such as impurities and deficiencies increase.[18] In the case of Hg-1201, the change of volume with respect to pressure is almost linear up to 10 GPa, which was also found by Novikov and co-workers.[10]

Furthermore, it can be seen from the data in Table II that for all compounds the change in the lattice parameters under pressure is quite different for different directions. In general, while going from ambient pressure to 15 GPa, a shrinks by about 4% while c decreases by about twice as much. This is in good agreement to experimentally found compressibilities.[19,20] It follows that the unit cell absorbs most of the pressure by shrinking the interlayer distance. A detailed study of the bond distances reveals that nearly the whole change in the c parameter is due to the change of the Cu-O^a bond, while the Hg-O^a bond is rigid, i.e., shows only very small change with applied pressure. Thus, a strong pressure dependence of the electronic states in the CuO_2 planes can be expected due to the enhanced interaction of copper with the apical oxygen. In the case of the compounds with $n=2,3$, and 4 the situation is similar. For these compounds we find that the CuO_2 planes are slightly buckled, in agreement with experiment.[15,18]

B. Band structures

The electronic structure of most members of the Hg-based cuprates has been studied in detail.[10–12,21–23] To investigate the dependence upon pressure, we calculated the band structures of Hg-1201, Hg-1212, Hg-1223, and Hg-1234 from 0 to 15 GPa. In Fig. 2 the band structure of Hg-1201 is depicted along several high-symmetry lines. Note that the band structure was plotted within a small energy region to make the features around the Fermi energy more visible. It can be seen that one band crosses the Fermi level E_F several times. This is a CuO_2 dominated band which is a characteristic for layered cuprates. It crosses the Fermi surface between X–M, M–Γ, R–A, and A–Z. The band maximum can be found at M and its minimum is located at Γ. The band width is about 3.91 eV under ambient pressure and increases to 4.44 eV under 15 GPa, which is an increase of almost 15%. A conduction band comes close to E_F at X and R. This band is found to have Hg-O^a character. Under pressure it crosses the Fermi level and causes hole doping of the half filled Cu^1($d_{x^2-y^2}$)-O^1 band. As pointed out in the preceding section, certain structural requirements concerning the Cu-O in-plane distance have to be fulfilled to make this hole doping possible. Furthermore, the saddle point of the valence band at X and R moves up under pressure. While, near the X point this saddle does not reach E_F, it crosses the Fermi level around R at about 12 GPa which is a somewhat smaller value compared to the estimation of Ref. 23.

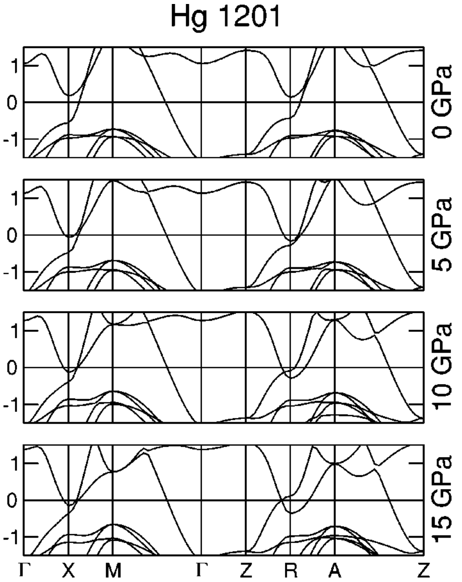

FIG. 2. Band structure of Hg-1201 along some high-symmetry lines for ambient pressure up to 15 GPa. The band structure is plotted with respect to the Fermi level and is measured in electron volt.

Figure 3 shows the band structure of the Hg-1212 compound. The similarity to the band structure of Hg-1201 is obvious. However, there are now two bands corresponding to the two CuO_2 planes, that cross the Fermi level. Both bands have their maximum at M and minimum at Γ. The band widths are similar to the Hg-1201 compound and grow from 3.92 eV under ambient pressure to 4.39 eV under 15 GPa. Furthermore, the Hg-O^a band almost touches the Fermi level at ambient pressure. This means that the hole doping of the Cu^1-O^1 already starts at ambient pressure. Similar to the one-

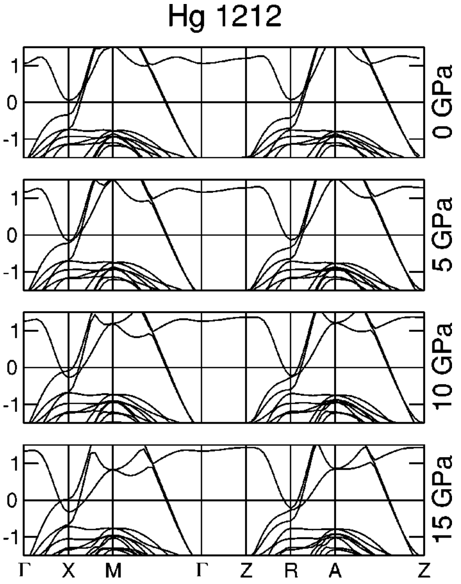

FIG. 3. Band structure of Hg-1212 along several high-symmetry lines for ambient pressure up to 15 GPa. Energies are given in electron volt and with respect to the Fermi energy.

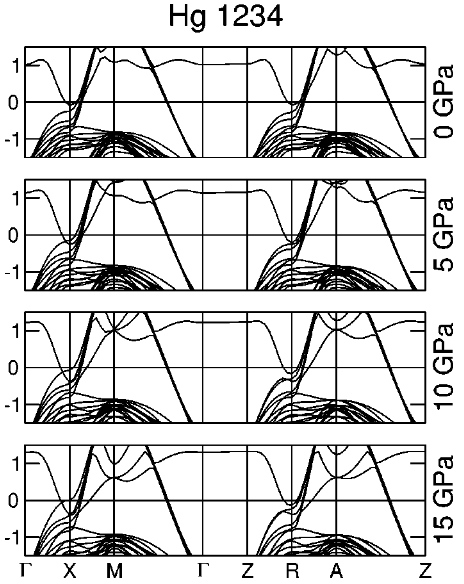

FIG. 5. Band structure of Hg-1234 along high-symmetry lines for ambient pressure up to 15 GPa. The band structure is given in electron volt and with respect to the Fermi level.

layered compound, this effect can be increased by applying pressure. At the same time the saddle points of the valence band at *X* and *R* move toward E_F. While, near *R* the saddle does not cross E_F, it reaches the Fermi level at *X* at 15 GPa. Note that, concerning the moving of this band, the points *X* and *R* are exchanged when going from the one-layered to the two-layered compound.

The band structure of Hg-1223 is plotted in Fig. 4. As for the previously discussed compounds, the important characteristics remain the same. It follows that now three CuO_2 bands cross the Fermi level. They are hole doped through the existence of the Hg-O^a band. The band characteristics and extrema are similar to systems already discussed, although the change in band widths is only about 8% and therefore the smallest of all four compounds. The pressure dependence is very similar to the Hg-1212 system: the saddle point in the valence band moves up and crosses the Fermi level at about 15 GPa at *R*. Note that, with respect to this moving, the *X* and *R* points are swapped again, so that the Hg-1223 system behaves similar to the Hg-1201 compound.

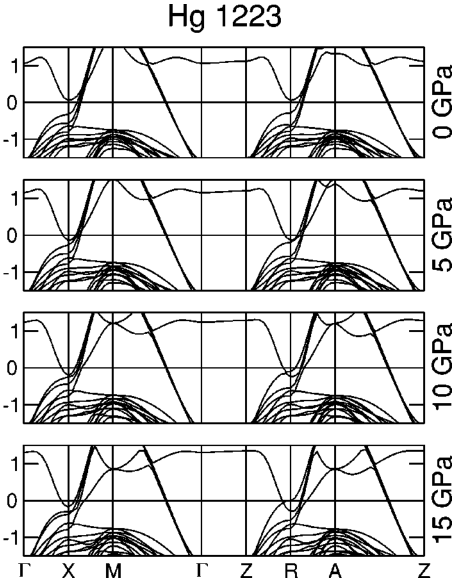

FIG. 4. Band structure of Hg-1223 along high-symmetry lines for ambient pressure up to 15 GPa. Energies are in electron volt and with respect to the Fermi energy.

Figure 5 depicts the band structure for the Hg-1234 system. As for all the other compounds, the general characteristic of the band structure remains the same. Besides the obvious similarity, now four CuO_2 bands cross the Fermi surface. Band extrema of these bands are also found at *M* and Γ and the band width changes by about 10% under pressure. Concerning the movement of the saddle point of the CuO_2 band, the *X* and *R* points are swapped again in comparison to Hg-1223 and the crossing of the saddle point occurs at about 15 GPa. The general behavior of the points where saddles of the CuO_2 bands come close to the Fermi energy under pressure is collected for all four compounds in Table III.

C. Partial charges

As discussed in Sec. III, the LAPW method permits an analysis of the charge density within the spheres with respect

TABLE III. Points in the BZ where the saddle point of the CuO_2 band moves toward the Fermi level (and eventually crosses it) when pressure is applied.

Compound	No. CuO_2 layers	Saddle point crossing E_F	Saddle point not crossing E_F
Hg-1201	1	*R*	*X*
Hg-1212	2	*X*	*R*
Hg-1223	3	*R*	*X*
Hg-1234	4	*X*	*R*

TABLE IV. Cu and O partial charges for the compounds Hg-1201, Hg-1212, Hg-1223, and Hg-1234 under pressure.

Pressure	Hg-1201		Hg-1212		Hg-1223				Hg-1234			
[GPa]	$Cu^1 d_{x^2-y^2}$	$O^1 p_x$	$Cu^1 d_{x^2-y^2}$	$O^1 p_x$	$Cu^1 d_{x^2-y^2}$	$O^1 p_x$	$Cu^2 d_{x^2-y^2}$	$O^2 p_x$	$Cu^1 d_{x^2-y^2}$	$O^1 p_x$	$Cu^2 d_{x^2-y^2}$	$O^2 p_x$
0	1.4336	0.7330	1.4419	0.7330	1.4421	0.7317	1.4386	0.7281	1.4413	0.7363	1.4380	0.7337
5	1.4141	0.7375	1.4283	0.7362	1.4320	0.7348	1.4337	0.7313	1.4290	0.7407	1.4363	0.7395
10	1.3945	0.7412	1.4178	0.7400	1.4235	0.7377	1.4308	0.7344	1.4227	0.7461	1.4375	0.7457
15	1.3866	0.7466	1.4137	0.7443	1.4207	0.7416	1.4317	0.7381	1.4220	0.7521	1.4413	0.7519

to the decomposition of the angular quantum numbers l and m. As pointed out, when charges are compared for different pressures while the sphere radii are kept constant, the interpretation becomes more complicated since the amount of charge lying within the spheres with respect to the total charge becomes larger. In other words: Under pressure the volume of the unit cell shrinks, however, since the sphere radii are kept constant, charge is pushed into the sphere and the partial charges in the sphere increase.

In Sec. IV A we found that some of the bonds are more easily compressible than others. In particular, the Hg-O^a distance stays approximately the same under pressure. This behavior is reflected in the partial charges Hg p_x, Hg p_z, and $O^a p_z$. For all systems the calculations show only a small increase of the Hg p_x and Hg p_z partial charges under pressure. The same is true for the $O^a p_z$ charge.

Table IV shows the partial charges $d_{x^2-y^2}$ and p_x of the copper and oxygen atoms for all four systems under pressure. The copper charge in all compounds show a decrease with pressure, which, for the one and two-layered compounds, is quite large. For the three and four-layer systems an average over the layers has to be taken. Note that this effect is observed despite the fact that due to the constant atomic sphere radii a bigger fraction of the charge moves inside the spheres under pressure. This suggests that the effect found is even slightly underestimated. The opposite trend is found for the oxygen atoms: increasing pressure increases the charges. This effect, however, is smaller than the decrease of the copper charges and originates in the problem of the constant sphere sizes mentioned above. Note also that a small sphere radius for oxygen had to be chosen throughout all calculations in order to handle the small bond lengths under pressure. Test calculations with bigger sphere sizes for oxygen showed that the effect indeed becomes smaller, which supports the idea that it mostly originates in the treatment of the sphere radii. Therefore, the increase in the partial oxygen charges cannot be interpreted as hole filling and the dominant effect is the hole creation by the copper charges. Another cross check for the trend mentioned above can be made by looking at the corresponding bands in the band structure: In the regions of the Brillouin zone where the CuO_2 band is partially depopulated when pressure is applied, it is dominated by the copper character, which explains the different behavior of Cu and O charges.

The dependence of the charges on the number of layers n shows the following behavior: The Cu charges increase by inserting up to three layers and then slightly drop again by going to four layers. Note that the increase is more pronounced for higher pressures. Although the number of pressure induced holes per copper atom is smaller for the higher layered compounds, the effect is still larger there due to the higher number of layers. The oxygen charges, on the other hand, do not show a strong dependence on n.

As mentioned in the introduction, parameters such as the number of layers, pressure, and doping influence the transition temperature. It is also well known that the dependence of the transition temperature on the hole concentration is a common rule for all superconducting complex copper oxides. With the help of the charge decomposition above, a comparison of how these parameters influence the charges in the CuO_2 planes can be made. A comparison of pressure and doping can be done for the single-layered compound, where doping has been studied recently.[24,25] For pressure, as well as for doping, the number of holes in the CuO_2 planes is increased. While pressure mainly affects the copper charges, in the case of doping the oxygen charges decrease also. The picture for comparing pressure and composition is similar. By going from one to two and three layers the amount of holes per copper atom is smaller, but due to more layers, the effect is still larger for the more layered compounds. Note that by inserting the fourth layer, the number of holes does not increase anymore. It follows that the number of holes induced by any of the three control parameters exhibits the same behavior as the transition temperature.[3] This is an direct indication of the correlation between the hole content and T_c.

V. CONCLUSIONS

We performed first-principles calculations on the Hg-based cuprate family $HgBa_2Ca_{n-1}Cu_nO_{2n+2}$. Thereby, we studied the effect of composition $n=1,2,3,4$ and pressure in the range from 0 to 15 GPa.

Our results for the structural data under ambient pressure for all four compounds are in good agreement with experiment. The trends for the lattice constants a and c under pressure compare well to experimentally found compressibilities. Also, at any pressure, important parameters such as bond lengths were found to be in the corresponding range necessary for the appearance of superconducting properties. The analysis of the band structures revealed the following behavior: In all four systems ($n=1,2,3,4$) we found a corresponding number of CuO_2 dominated bands crossing the Fermi level, which is characteristic for layered cuprates. Furthermore, a conduction band comes close to E_F, which is found to have Hg-O^a character. Under pressure it crosses the Fermi level and causes hole doping of the half filled $Cu^1(d_{x^2-y^2})$-O^1 band. This mechanism is responsible for the creation of holes in the CuO_2 planes. Our analysis for the dependence of the hole concentration upon parameters such as pressure and the number of layers shows that a direct correlation between the hole content and the superconducting transition temperature exists.

ACKNOWLEDGMENTS

This work was funded by NSF Grant No. DMR-02-05125 and by the Austrian Science Fund, Project Nos. P13430 and P14004. Most of the calculations were done at the Materials Simulation Center, a Penn-State MRSEC and MRI facility. We also acknowledge financial support from the Heinrich-Jörg-Stiftung.

---

[1] A. Schilling, M. Cantoni, J.D. Guo, and H.R. Ott, Nature (London) **363**, 56 (1993).

[2] S.N. Putilin, E.V. Antipov, O. Chmaissem, and M. Marezio, Nature (London) **362**, 226 (1993).

[3] L. Gao, Y.Y. Xue, F. Chen, Q. Xiong, R.L. Meng, D. Ramirez, C.W. Chu, J.H. Eggert, and H.K. Mao, Phys. Rev. B **50**, 4260 (1994).

[4] S.M. Loureiro, E.V. Antipov, J.L. Tholence, J.J. Capponi, O. Chmaissem, Q. Huang, and M. Marezio, Physica C **217**, 253 (1993).

[5] E.V. Antipov, A.M. Abakumov, and S.N. Putilin, Supercond. Sci. Technol. **15**, 31 (2002).

[6] E.V. Antipov, S.M. Loureiro, C. Chaillout, J.J. Capponi, P. Bordet, J.L. Tholence, S.N. Putilin, and M. Marezio, Physica C **215**, 1 (1993).

[7] B.A. Scott, E.Y. Suard, C.C. Tsuei, D.B. Mitzi, T.R. McGuire, B.H. Chen, and D. Walker, Physica C **230**, 239 (1994).

[8] E.M. Kopnin, E.V. Antipov, J.J. Capponi, P. Bordet, C. Chaillout, S. de Brion, M. Marezio, A.P. Bobylev, and G. van Tendeloo, Physica C **243**, 239 (1994).

[9] C.W. Chu, L. Gao, F. Chen, Z.J. Huang, R.L. Meng, and Y.Y. Xue, Nature (London) **365**, 323 (1993).

[10] D.L. Novikov, M.I. Katsnelson, J. Yu, A.V. Postnikov, and A.J. Freeman, Phys. Rev. B **54**, 1313 (1996).

[11] D.J. Singh, Physica C **212**, 228 (1993).

[12] D.J. Singh and W.E. Pickett, Phys. Rev. Lett. **73**, 476 (1994).

[13] B.A. Hunter, J.D. Jorgensen, J.L. Wagner, P.G. Radaelli, D.G. Hinks, H. Shaked, R.L. Hitterman, and R.B. Von Dreele, Physica C **221**, 1 (1994).

[14] P.G. Radaelli, J.L. Wagner, B.A. Hunter, M.A. Beno, G.S. Knapp, J.D. Jorgensen, and D.G. Hinks, Physica C **216**, 29 (1993).

[15] A.R. Armstrong, W.I.F. David, I. Gameson, P.P. Edwards, J.J. Capponi, P. Bordet, and M. Marezio, Phys. Rev. B **52**, 15 551 (1995).

[16] P. Blaha, K. Schwarz, G. K. H. Madsen, D. Kvasnicka, and J. Luitz, *WIEN2k, An Augmented Plane Wave + Local Orbitals Program for Calculating Crystal Properties* (Technische Universität, Vienna, 2001).

[17] J.P. Perdew and Y. Wang, Phys. Rev. B **45**, 13 244 (1992).

[18] R. Gatt, E. Olsson, A. Morawski, T. Lada, A. Paszewin, I. Bryntse, A.M. Grishin, Yu. Eeltsev, P. Berastegui, and L.-G. Johansson, Physica C **276**, 270 (1997).

[19] J.H. Eggert, J.Z. Hu, H.K. Mao, L. Beauvais, R.L. Meng, and C.W. Chu, Phys. Rev. B **49**, 15 299 (1994).

[20] V. L Aksenov, A.M. Balagurov, B.N. Wsavenko, D.V. Sheptyakov, V.P. Glazkov, V.A. Somenkov, S.Sh. Shilshtein, E.V. Antipov, and S.N. Putilin, Physica C **275**, 87 (1997).

[21] D.L. Novikov and A.J. Freeman, Physica C **212**, 233 (1993).

[22] C.O. Rodriguez, N.E. Christensen, and E.L. Peltzer y Blanká, Physica C **216**, 12 (1993).

[23] D.L. Novikov, O.N. Mryasov, and A.J. Freeman, Physica C **222**, 38 (1994).

[24] C. Ambrosch-Draxl, P. Süle, H. Auer, and E.Ya. Sherman, Phys. Rev. B **67**, 100505(R) (2003).

[25] C. Ambrosch-Draxl, E. Ya. Sherman, H. Auer, and T. Thonhauser, J. Supercond. **17**, 215 (2004).